

Document downloaded from:

<http://hdl.handle.net/10251/150661>

This paper must be cited as:

Garzón-Roca, J.; Capa-Guachon, VE.; Torrijo, F.; Company Rodríguez, J. (2019). Designing Soil-Nailed Walls Using the Amherst Wall Considering Problematic Issues during Execution and Service Life. *International Journal of Geomechanics*. 19(7):1-14.  
[https://doi.org/10.1061/\(ASCE\)GM.1943-5622.0001453](https://doi.org/10.1061/(ASCE)GM.1943-5622.0001453)



The final publication is available at

[https://doi.org/10.1061/\(ASCE\)GM.1943-5622.0001453](https://doi.org/10.1061/(ASCE)GM.1943-5622.0001453)

Copyright American Society of Civil Engineers

Additional Information

# DESIGNING SOIL NAILED WALLS CONSIDERING PROBLEMATIC ISSUES DURING EXECUTION AND SERVICE LIFE BY THE AMHERST WALL.

Julio Garzón-Roca<sup>a,\*</sup>, Vicente Capa<sup>b</sup>, F. Javier Torrijo<sup>c</sup>, Julio Company<sup>d</sup>

<sup>a</sup> Assistant Professor, Department of Geotechnical Engineering, Universitat Politècnica de València, Camino de Vera s/n, 46022, Valencia, Spain.

<sup>b</sup> Graduate Student, Department of Construction Engineering and Civil Engineering Projects, Universitat Politècnica de València, Camino de Vera s/n, 46022, Valencia, Spain.

<sup>c</sup> Associate Professor, Department of Geotechnical Engineering, Universitat Politècnica de València, Camino de Vera s/n, 46022, Valencia, Spain.

<sup>d</sup> Assistant Professor, Department of Geotechnical Engineering, Universitat Politècnica de València, Camino de Vera s/n, 46022, Valencia, Spain.

\*Corresponding author. Tel.: +34 963 877 583; fax: +34 963 877 569; E-mail address: jugarro@upv.es

## Abstract

Soil nailing is a technique commonly used as temporary or permanent earth retention system in soft soils. Habitually the design of a soil nailing focuses on its performance at failure, computing a safety factor, and thus neglecting ground deformations. In this paper, an analysis and comparison of the convenience of the use of the limit equilibrium method and the finite element method for designing a soil nailing is conducted. The assessment considers both the suitability of an easy and fast design process, and the necessity to take into account issues such as ground deformations to avoid problematic consequences that can arise during their execution phase and service life. For performing the analyses a numerical study of the “Amherst wall”, a full-scale soil nailed wall built to be an experimental test in last years of the twentieth century, is carried out. A two-step process for designing soil nailed walls is proposed. The first step involves the use of limit equilibrium methods to define the main parameters. The second step deals with the development of a finite element model to consider ground deformations as well as to determine nail forces. An approach based on the use the Mohr-Coulomb model for simulating materials more similar to granular soils and the Hardening Soil model for simulating materials more similar to cohesive soils is also presented in the paper as an answer to numerically model soil-nailed walls in ground situations where the soil is neither pure cohesive nor pure granular.

**Keywords:** Soil nailing; Performance at failure; Ground deformations; Execution phase; Service life; Numerical simulation; Finite element modelling; Limit equilibrium method.

31 **Introduction**

32 Soil nailing is a low cost, easy construction and common technique used all over the world for enhancing the  
33 stability of retaining walls, slopes, and excavations, and it is usually used for temporary or permanent earth  
34 retention (Yuan et al. 2003; Holman and Tuozzolo 2009; Ghareh, 2015). Basically, soil nailing is an in situ  
35 ground reinforcement technique which consists of introducing a series of reinforcing elements, i.e. nails, into  
36 the existing ground with the aim of adding the resistance of those elements to the shear strength of the in-situ  
37 ground (Junaideen et al. 2004; Pradhan et al. 2006; Yin and Su 2006; Su et al. 2007; Xue et al. 2011; Seo et  
38 al. 2014).

39 In contrast to anchors and tiebacks (Ehrlich and Silva 2015), nails are passive elements which are not post-  
40 tensioned after installation and only mobilize their reinforcing effect when ground movements occur  
41 (Sheahan 2000; Sheahan and Ho 2003). Nails are subjected mainly to tension forces but may develop shear  
42 forces and resist bending moments when are oriented counterclockwise to the normal direction of the slip  
43 surface (Fan and Lou 2008; Ghareh 2015). Reinforcing bars, i.e. rebar, are normally used as nails, but hollow  
44 steel section or even solid bars could also be used.

45 Installation of a soil nailing in an existing ground typically involves conducting a relatively small excavation  
46 which remains stable without any retaining system, drilling a row of holes in the slope face, inserting the nail  
47 elements and then bonding the nails and the ground by grouting. A shotcrete is normally casted at the slope  
48 face to unify the nails, create a uniform surface and work as a retaining system at local scale. This procedure  
49 may continue until reaching the total depth of the excavation, building a “soil nailed wall”.

50 Designing of a soil nailed wall, generally focuses on its performance at failure, which is commonly  
51 translated into fulfilling a given value of the safety factor (defined as the ratio of the forces that contribute to  
52 stabilize the system to the forces that tend to make it unstable). However, ground deformations are not taken  
53 into account in the referred safety factor. Ground deformations may give rise to problems in surrounding  
54 buildings and structures (Tan et al. 2015) and may also endanger the safety of the own excavation due to  
55 excessive movements of the slopes. Consequently, even though a soil nailed wall fulfills a safety factor it  
56 does not necessarily means that the system is properly designed.

57 This paper presents an analysis and comparison of the use of limit equilibrium methods and finite element  
58 methods for designing a soil nailed wall. Even though different numerical methods were developed (Kim et

59 al. 1997; Sivakumar Babu et al. 2002; Yuan et al. 2003; Liu et al. 2016), nowadays limit equilibrium  
60 methods and finite element methods are most commonly used when analyzing this kind of earth retention  
61 structures (Smith and Su 1997; Zhang et al. 1999; FHWA 2003; Yuan et al. 2003; Fan and Luo 2008; Singh  
62 and Sivakumar Babu 2010; Wei and Cheng 2010; Ghareh 2015). The assessment conducted considers both  
63 the suitability of an easy and fast design process, and the necessity to take into account issues such as ground  
64 deformations to avoid problematic consequences that can arise during their execution phase and service life.  
65 For doing this, a numerical study of the soil nailed structure “Amherst wall” is carried out (Sheahan 2000).  
66 This is one of the few existing full-scale soil nailed walls built to be an experimental test, along with the test  
67 conducted in 1986 for the French national research project “Clouterre” (Plumelle et al. 1990). There exist  
68 some examples of instrumented soil nailed walls (Holman and Tuozzolo 2009; Wood et al. 2009), but these  
69 are normally real infrastructures, so failure is generally not occurring. On the other hand, the Amherst wall  
70 was led deliberately to failure, which enables the study of a soil nailed wall at collapse. Two models of the  
71 Amherst wall using the finite element method and limit equilibrium method, respectively, are built, and an  
72 analysis in terms of performance at failure, load distribution patterns developed in the nails and ground  
73 deformations issues is undertaken so as to establish the convenience of using each of the methods under  
74 study.

## 75 **The Amherst wall**

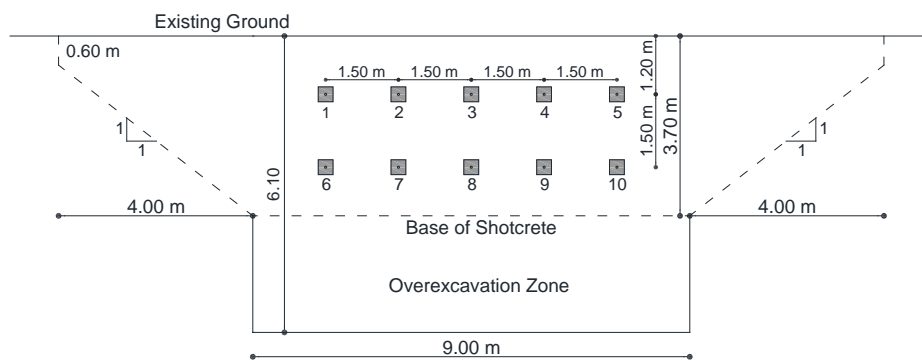
### 76 *General description*

77 The “Amherst wall” was built in 1997 at the University of Massachusetts-Amherst (UMass-Amherst)  
78 National Geotechnical Experimentation Site (NGES), near the town of Amherst, Massachusetts. This was a  
79 full-scale soil nailed wall built as an experimental test carried out to increase the knowledge about the soil  
80 nailing technique.

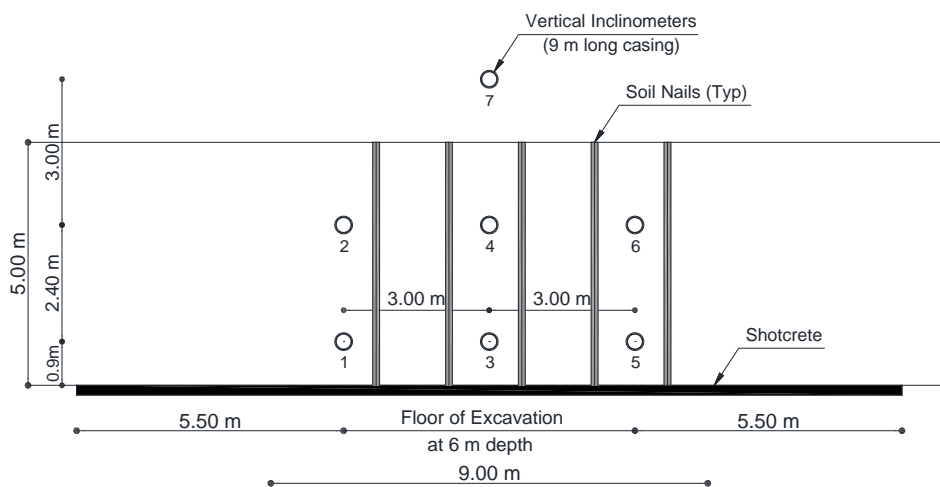
81 The Amherst wall reproduced a typical excavation in a soft soil using the soil nailing technique. Excavation  
82 of the ground was made in three main phases. The first excavation phase reached around 2.5 m; the second  
83 excavation phase reached a total depth of 3.6 m. After each excavation phase, a series of nails were installed  
84 in the ground, the vertical slope face was shotcreted and the head of the nails were hand-tightened. The third  
85 excavation phase corresponded to an overexcavation (no nail or shotcrete was installed), and was carried out

86 until the failure of the wall. Works were developed from August 18th, 1997 to September 7th, 1997 (Oral  
 87 and Sheahan 1998). More information about the construction process can be found in Sheahan (2000).

88 **Figs. 1 and 2** show the wall's front elevation (**Fig. 1a**), plan view (**Fig. 1b**) and side cross-section (**Fig. 2a**)  
 89 of the Amherst wall. As observed, two rows of nails were installed. Both rows had a total of 5 nails separated  
 90 1.5 m from each other. The first row of nails was located 1.2 m from the top of the slope. The second row  
 91 was located 1.5 m from the first row (so at a depth of 2.7 m). Nails consisted of 19-mm-diameter steel bars  
 92 of 414 MPa of yield stress, placed with an inclination of 20° below horizontal. The shotcrete facing was 100  
 93 mm thick and 100 mm x 100 mm welded wire fabric was used as reinforcement. Besides, some  
 94 instrumentation was installed in the Amherst wall, especially a total of 7 vertical inclinometers reaching a  
 95 depth of 9.1 m and which were used to monitor lateral ground deformations. It is important to mention that  
 96 no significant groundwater was observed during the excavation (Sheahan 2000).



(a)

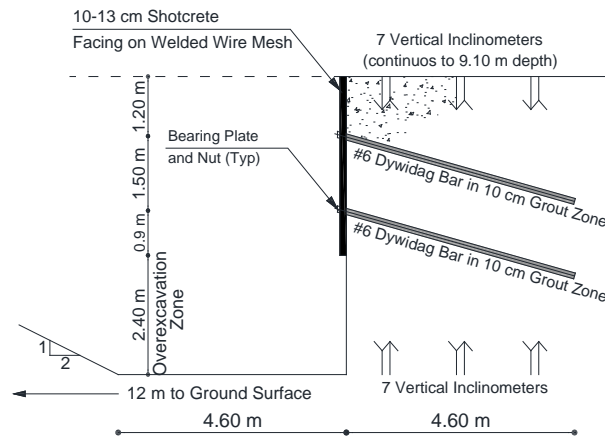


(b)

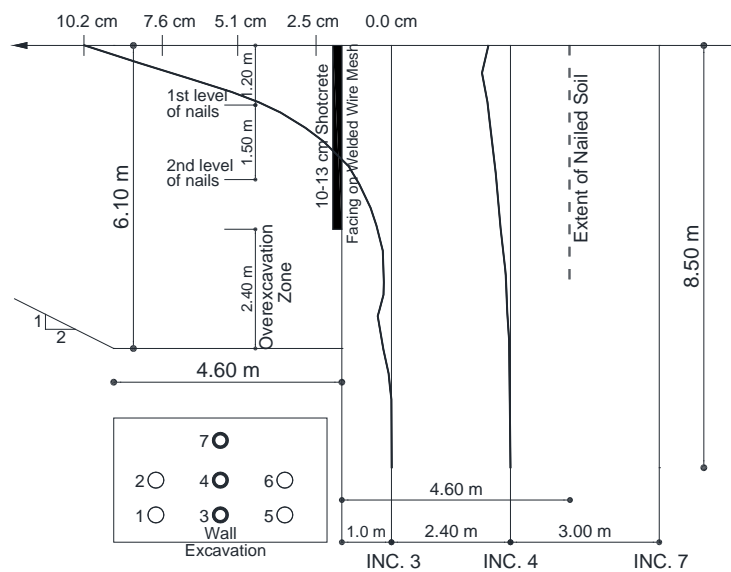
97

98

*Fig. 1. The Amherst wall front elevation (a) and plan view (b). Modified form Sheahan 2000.*



(a)



(b)

99

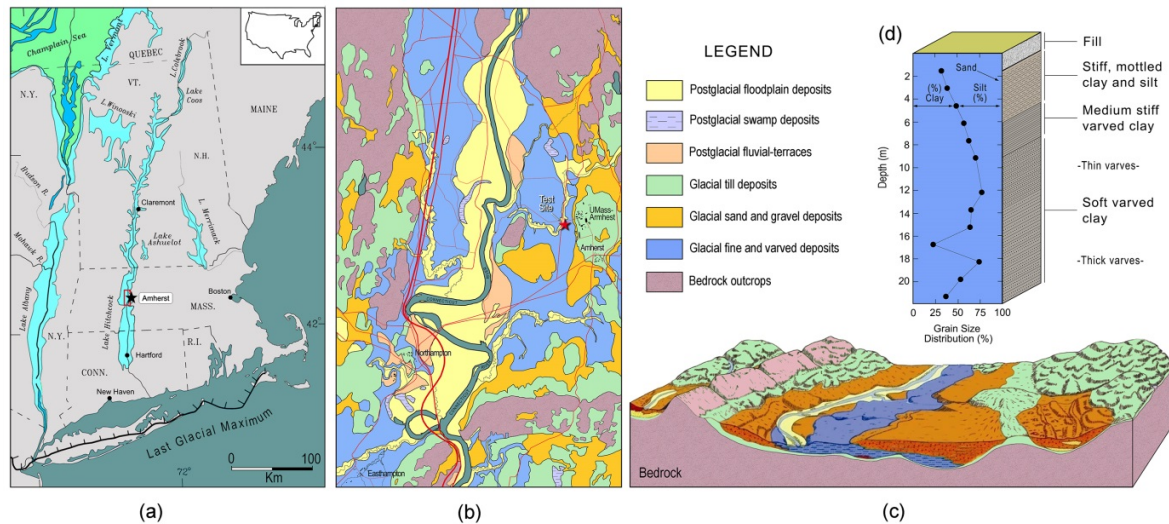
100 *Fig. 2. Amherst wall cross-section (a) and lateral deformation (b) recorded by the inclinometers placed at*  
 101 *the middle section of the wall, i.e. inclinometers 3, 4 and 7. Modified from Sheahan 2000.*

102 *Geological-geotechnical characterization of the area*

103 The site is situated within the Connecticut River Valley (**Fig. 3a**), approximately 1.5 km within the shore of  
 104 the ancient Glacial Lake Hitchcock, the large pro-glacial lake system that occupied the length of the upper  
 105 Connecticut River Valley in central New England (Stone and Ashley 1995; DeGroot and Lutenecker 2005).

106 A thick deposit of varved lake-bottom silts and clays (Ridge et al. 2012), locally referred to as Connecticut  
 107 Valley Varved Clay (CVVC), was deposited on the floor of the glacial lake basin, meanwhile coarse deposits  
 108 (i. e. sand and gravels) and meteoric-stream-fed deltas were graded to its shorelines. The postglacial deposits

109 partly overlie the Paleocene glaciolacustrine ones. They consist of stream-terraces, floodplain and swamp  
 110 deposits, fluvial-estuarine channel-fills, eolian dunes, beaches, and marine delta deposits (Stone et al. 1998;  
 111 Thorson et al. 2014). At present, the Connecticut River generally follows the course of the ancient Lake  
 112 Hitchcock so, as expected modern fluvial deposits also cover the glaciolacustrine lake-bottom sediments  
 113 (Fig. 3b-c).



114 (a) 115 *Fig. 3. Geological setting of the Amherst test wall: (a) Location of Glacial Lake Hitchcock in New England*  
 116 *and nearby contemporaneous glacial lake systems (rectangle shows the position of the figure 2b); (b)*  
 117 *Simplified geological map of the Connecticut River Alluvial Lowland showing the location of the UMass*  
 118 *Amherst NGES (star). Block diagram illustrating the distribution of glacial and postglacial deposits*  
 119 *overlying bedrock in the Connecticut River Valley; (d) General soil profile and grain distribution at the*  
 120 *UMass Amherst NGES site ((a), (c) and (d) modified from Ridge and Larsen, 1990; Stone et al., 1998; and*  
 121 *Woods, 1995; DeGroot and Lutenegeer, 1995, respectively).*

122 The soil stratigraphy at the UMass Amherst NGES test site is well-documented. Cores drilled to bedrock in  
 123 the clayey soils reached a maximum depth of exploration of about 24.4 m (Woods 1995). However, nearby  
 124 borings have yielded a 33 m-thick sequence. In both cases, samples are mainly dominated by the lake-bottom  
 125 varved deposits of the former Glacial Lake Hitchcock (Brigham-Grette et al. 2000).

126 The sedimentary sequence at the test site begins with an uppermost compacted crust of miscellaneous fine-  
 127 grained and granular fill, altered by soil development, extending from the surface to about 1.2 to 1.5 m. The  
 128 fill consist of CVVC placed about 30 years ago after excavations at the Amherst Wastewater Treatment  
 129 plant, which is adjacent to the site (Beim and Luna 2012). At 1.5 m depth, there is a gradational transition

130 from the abovementioned stiff silty-clay fill to a new layer of thin (< 1 cm), poorly defined varved clays.  
131 This transitional unit (about 20 cm thick) commonly also contains thin (1-2 mm) discontinuous, interbedded  
132 clay sheets. These upper horizons are underlain by more than 30 m of CVVC. The upper 5 to 6 m of this  
133 deposit is overconsolidated. Below the varved silt and clays are lightly to normally consolidated, increasing  
134 consolidation with depth (DeGroot and Lutenegeger 1994). **Fig. 3d** shows a simplified vertical profile of the  
135 site.

136 A vertical anisotropy of the varved deposit have undergone significant changes as a result of pedogenic  
137 alteration, human activity and weathering. This zone, commonly known as a crust, extends to about 5 to 6 m  
138 below ground surface, near the maximum depth of the excavation of the Amherst test wall. According to  
139 Sheahan (2000), in that area plasticity index varies from 17 to 22% while undrained strength ranges from 80  
140 kPa to less than 40 kPa.

141 The consistence properties of the varved clays also varies seasonally in the upper portion of the profile: the  
142 ground water table at the UMass Amherst NGES test site usually occurs in the upper 2-3 meters below  
143 ground surface, but varies as much as 1 to 2 m throughout the year according with seasonal groundwater  
144 recharge (DeGroot and Lutenegeger 1994, 2005).

#### 145 *Failing of the wall and lateral deformation*

146 Failure of the Amherst wall due to the overexcavation occurred after overexcavating 2.4 m, i.e. when a total  
147 depth of 6 m was attained. Global failure took place during the night of September 7th, apparently initiated  
148 by soil sloughing from the overexcavation face (Sheahan 2000). **Fig. 2b** displays the lateral deformation  
149 recorded by those inclinometers placed at the middle section of the wall (inclinometers 3, 4 and 7 in **Fig. 1b**)  
150 at failure.

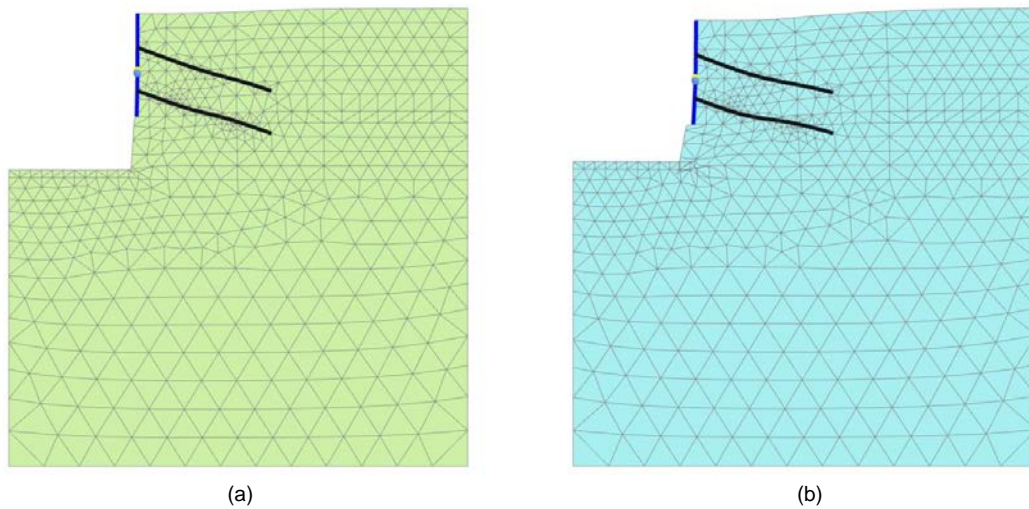
#### 151 **Numerical study**

##### 152 *General approach*

153 The analysis of the geological-geotechnical characteristics of the soil where the Amherst wall was built  
154 revealed a very heterogenic soil, formed by sand, silt and clay, with different proportion of each component  
155 at different depths. Besides, geotechnical parameters were also very variable, specially undrained shear  
156 strength which ranged from 80 kPa at the upper layers to 40 kPa or less at the lower layers.



157 Nevertheless previous analytical studies based on limit equilibrium methods (Sheahan 2000; Sheahan and Ho  
158 2003) considered that soil to be a uniform undrained cohesive material. However, when this kind of material  
159 is tried to model by the finite element method (see **Fig. 4**), it is easy to observe that deformations of the  
160 nailed wall are completely different as in reality (rotation of the wall by its upper part occurred in a  
161 numerical model instead of rotation by its lower part seen experimentally).



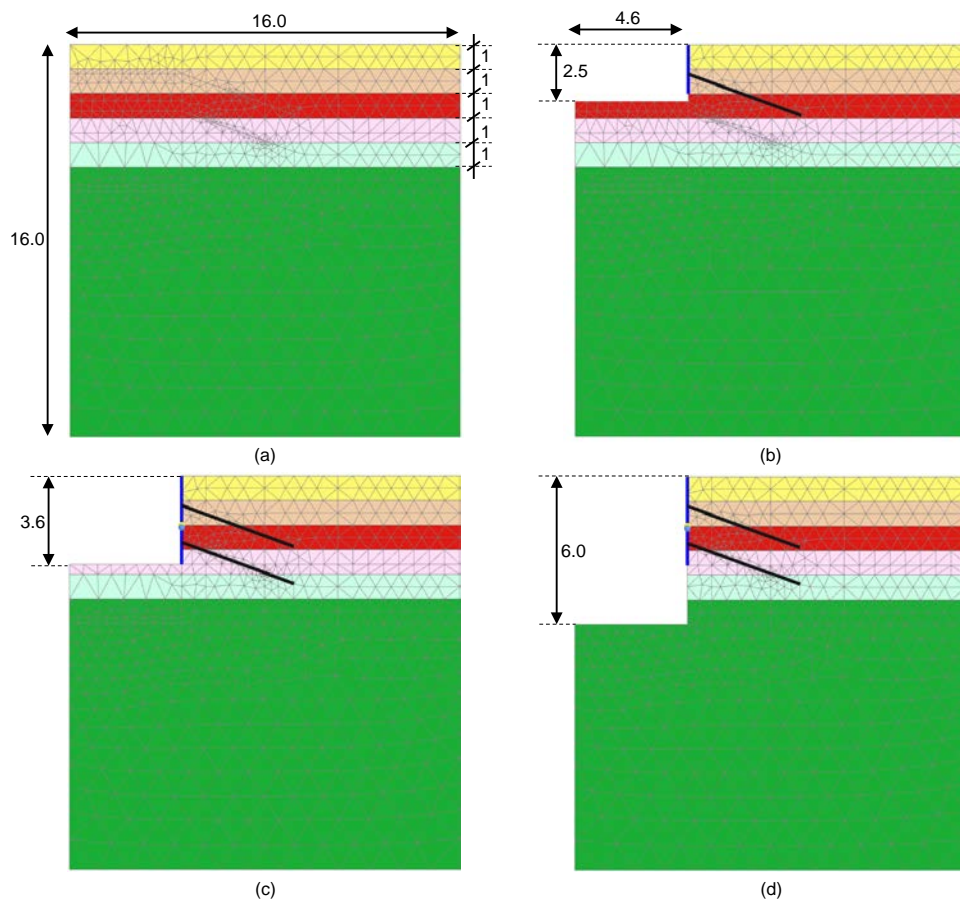
162 (a) (b)

163 *Fig. 4. Deformed shapes of the Amherst wall obtained by a finite element simulation considering a unique*  
164 *undrained cohesive soil (approach followed previously by Sheahan 2000 and Sheahan and Ho, 2003). Soil*  
165 *was modelled using the Mohr-Coulomb model (a) and the Hardening Soil model (b). It is observed that in*  
166 *both cases rotation of the wall occurs by its upper part instead of rotation by its lower part, as seen*  
167 *experimentally. The finite element simulations where conducted following the same approach as that*  
168 *described in this paper.*

169 Hence, a back-analysis was conducted in this paper in order to reproduce as close as possible the behavior  
170 observed in the Amherst wall. Both a finite element model and a limit equilibrium method model were  
171 developed. Due to the natural variation observed in the ground characteristics at the depths where the wall  
172 was built, the ground was numerically stratified each meter until reaching 5 m (i.e. one meter before the total  
173 excavation). From that point, a uniform material was considered. In both cases, nails and shotcrete were  
174 placed at the same positions as they were located in the experimental test and a uniform value of 18.9 kN/m<sup>3</sup>  
175 was taken as unit weight of the soil. Water table did not appear during the excavations performed. Thus, no  
176 water table was introduced in the numerical models (i.e. pore water pressure was null).

178 The finite element commercial software Plaxis 2D v.2016 (PLAXIS 2016) was used to build a numerical  
 179 model of the Amherst wall. A generic cross section of the wall was selected to be simulated in plane strain  
 180 (Shiu et al. 2006; Fan and Luo 2008; Singh and Sivakumar Babu 2010). The model developed tried to  
 181 simulate the Amherst wall behavior at failure, taking into account the construction process.

182 A total area of 16x16 m (see **Fig. 5a**) was modelled to avoid any disturbance in the results due to the  
 183 proximity of the model boundaries to the area of interest. The nailed wall was located 4.6 m from the left  
 184 border of the model, leaving the same excavation space as in reality (see **Fig. 2a and Fig. 5b**). More than 10  
 185 m of ground from the wall to the right border was left, space enough to introduce the nails and to study its  
 186 influence. **Fig. 5** shows the numerical model developed.



187  
 188 *Fig. 5. Finite element model developed for studying the Amherst wall (dimensions in m): (a) Model prior to*  
 189 *any excavation; (b) Model after conducting the first excavation and installing the first row of nails (and*  
 190 *shotcrete); (c) Model after conducting the second excavation and installing the second row of nails (and*  
 191 *shotcrete); (d) Model after conducting the overexcavation.*

192 The finite element software Plaxis v.2016 allows defining different stages to simulate the construction  
 193 process of an infrastructure. It is possible, in any stage, to remove ground clusters to reproduce an excavation  
 194 or add structural elements such as the nails and the shotcrete face. Hence, to study the Amherst wall a total of  
 195 six stages were considered: (i) initial state (no excavation takes place, ground is in its natural state); (ii)  
 196 excavation of the first 2.5 m; (iii) installation of the first row of nails and building of the shotcrete face from  
 197 the top until the bottom of the excavation; (iv) excavation until reaching a depth of 3.6 m; (v) installation of  
 198 the second row of nails and building of the shotcrete face until the bottom of the new excavation; (vi)  
 199 overexcavation until reaching a depth of 6 m.

200 Soil was meshed using 6-node triangular isoparametric elements with three Gauss points for each element,  
 201 while nails and shotcrete were introduced as plate elements, with flexural rigidity and normal stiffness, and  
 202 meshed with 3-node elements, with three degrees of freedom per node (two translational and one rotational).  
 203 A connection element was introduced between the shotcrete casted before and after the construction stage  
 204 (v), which allowed free rotation (no bending moment resisted). That was conducted trying to reproduce the  
 205 clear change of deformation seen experimentally (see **Fig. 2b**) in the nailed wall.

206 Both the nails and the shotcrete were modelled using an elastic behavior. Mechanical values used for nails  
 207 and shotcrete were obtained based on the material properties and the geometry of these elements, and are  
 208 given in **Table 1**. Due to their discrete nature, nails were modelled using an “equivalent plate model”  
 209 approach (Al-Hussaini and Johnson 1978; Unterreiner et al. 1997; Singh and Sivakumar Babu 2010),  
 210 replacing them by a plate extended to one unit width. Particularly, normal stiffness ( $EA$ ) and flexural rigidity  
 211 ( $EI$ ) of the nails were computed as:

$$212 \quad EA = \frac{E_{eq}}{s_h} \cdot \left( \frac{\pi \cdot D_{dh}^2}{4} \right) \quad (1)$$

$$213 \quad EI = \frac{E_{eq}}{s_h} \cdot \left( \frac{\pi \cdot D_{dh}^4}{64} \right) \quad (2)$$

214 where  $s_h$  is the horizontal spacing of soil nails,  $D_{dh}$  the diameter of the drill hole and  $E_{eq}$  the equivalent elastic  
 215 modulus of the grouted soil nail, which is given by:

$$216 \quad E_{eq} = E_n \cdot \left( \frac{A_n}{A} \right) + E_g \cdot \left( \frac{A_g}{A} \right) \quad (3)$$

217 with:

$$218 \quad A = 0.25 \cdot \pi \cdot D_{dh}^2 \quad (4)$$

$$219 \quad A_n = 0.25 \cdot \pi \cdot d^2 \quad (5)$$

220 being  $A$  the total cross-section area of grouted soil nail, given by the diameter of the drill hole,  $D_{dh}$ ;  $E_n$  and  $A_n$   
 221 the elastic modulus and cross-section area of the steel nails (with  $d$  the diameter of the steel bar),  
 222 respectively; and  $E_g$  and  $A_g$  the elastic modulus and area of the grout material (note that  $A_g = A - A_n$ ).

223 *Table 1. Mechanical characteristics of the shotcrete and nails as plate elements.*

Element	Weight (kN/m / m)	$E$ (GPa)	$EA$ <sup>1,2</sup> (kN / m)	$EI$ <sup>1,2</sup> (kN·m <sup>2</sup> / m)	$\nu$
Shotcrete	2.70	34.5	$3.45 \cdot 10^6$	2875.0	0.2
Nails	0.13	200	$117.9 \cdot 10^3$	76.67	0.3

<sup>1</sup> Values of  $EA$  and  $EI$  for shotcrete were computed as:

$$EA = E_c \cdot t_s ; EI = E_c \cdot \frac{t_s^3}{12}$$

Being  $E_c$  the elastic modulus of the shotcrete and  $t_s$  the shotcrete thickness. Values for those parameters were taken based on the work of Sheahan (2000) and Sheahan and Ho (2003).

<sup>2</sup> Values of  $EA$  and  $EI$  for nail were computed as:

$$EA = \frac{E_{eq}}{s_h} \cdot \left( \frac{\pi \cdot D_{dh}^2}{4} \right) ; EI = \frac{E_{eq}}{s_h} \cdot \left( \frac{\pi \cdot D_{dh}^4}{64} \right) \text{ with } E_{eq} = E_n \cdot \left( \frac{A_n}{A} \right) + E_g \cdot \left( \frac{A_g}{A} \right) ; A = 0.25 \cdot \pi \cdot D_{dh}^2 ; A_n = 0.25 \cdot \pi \cdot d^2$$

Being  $s_h$  the horizontal spacing of soil nails,  $D_{dh}$  the diameter of the drill hole,  $d$  the diameter of the steel bar (nail) and  $E_n$  and  $E_g$  the elastic modulus of the nail and the grout material that fills the drill hole, respectively. Values for those parameters were taken based on the work of Sheahan (2000) and Sheahan and Ho (2003).

224

225 Regarding the soil elements, two possible mechanical behaviors were taken into account in the modelling  
 226 process: the well-known Mohr-Coulomb model (Kim et al. 1997; Smith and Su 1997; Zhang et al. 1999;  
 227 Sivakumar Babu et al. 2002; Fan and Luo 2008) and the Hardening Soil model (Liew and Khoo 2006; Singh  
 228 and Sivakumar Babu 2010). The former consists of an elastic part based on Hooke's law of isotropic  
 229 elasticity (defined by the elastic modulus,  $E$ , and the Poisson ratio,  $\nu$ ) and a plastic part based on the Mohr-  
 230 Coulomb failure criterion, which depends on cohesion,  $c$ , and the angle of friction,  $\phi$ , and formulated in a  
 231 non-associated plasticity framework (the plastic potential function also depends on the dilatancy angle,  $\psi$ ).  
 232 The latter is based on the observed hyperbolic relationship between the deviatoric stress and the axial  
 233 deformation in a cohesive soil element, where the Mohr-Coulomb failure criterion (defined by  $c$  and  $\phi$ ) set  
 234 the maximum deviatoric stress withstood by the soil element. In this model, rigidity is not constant but it

235 depends on the stress level, so the elastic modulus  $E_{50}$  corresponding to the stiffness of the soil when  
236 deviatoric stress is half the maximum one is used. Additionally, the oedometric modulus,  $E_{oed}$ , is taken into  
237 account and rigidity of the soil under unloading-reloading is considered by the modulus  $E_{ur}$ . Relation  
238 between volumetric plastic deformation and shear plastic deformation is considered by the dilatancy angle,  
239  $\psi$ . The normally consolidated earth pressure at rest coefficient  $K_{0,nc}$  is the last parameter needed by the  
240 Hardening Soil model. More information about this model along its verification may be found in Schanz et  
241 al. (1999).

242 Both the Mohr-Coulomb model and the Hardening Soil model allow an undrained or drained behavior of the  
243 soil. The Mohr-Coulomb model represents the behavior of geotechnical materials in a general way and it is  
244 optimal to model granular material. Unfortunately, it does not include stress-dependency, stress-path  
245 dependency, strain dependent stiffness, or anisotropic stiffness, which may be a downside when modelling  
246 cohesive materials. Conversely, the Hardening Soil model is a more advanced model for the simulation of  
247 soil behavior and described the soil stiffness much more accurately. This is a good model for simulating  
248 cohesive materials but it involves a total of 11 parameters instead of the 6 parameters used in the Mohr-  
249 Coulomb model.

#### 250 *Limit equilibrium methods*

251 The commercial software Slide v.7 (RocScience 2017) was used to perform a stability analysis of the  
252 Amherst wall by limit equilibrium methods. These methods consider only the static mechanical laws to  
253 define the stability of a soil slope, neglecting the deformation of the ground, and assuming that the shear  
254 strength of the soil is totally and simultaneously developed along the sliding surface. The most common way  
255 of applying limit equilibrium methods is by the method of slices, which divides the sliding mass into a  
256 number of vertical slices to solve the problem, assuming that failure of the soil is governed by the Mohr-  
257 Coulomb criterion, slices behave as rigid bodies and no stresses exist inside each slice.

258 Safety of the slope is defined as the ratio between the available shear strength in the sliding surface,  $S_m$ , and  
259 the needed one to keep a strict equilibrium of the sliding mass. That ratio is known as safety factor,  $F$ .  
260 Hence, since failure follows Mohr-Coulomb criterion, value of available shear strength on each slide is given  
261 by:

262 
$$S_m = \frac{c \cdot l}{F} + N \cdot \frac{\tan \phi}{F} \quad (6)$$

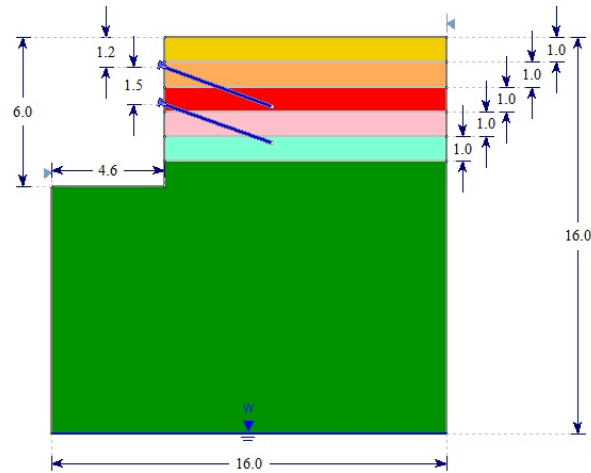
263 being  $c$  the material cohesion and  $\phi$  its angle of friction,  $l$  the length of the sliding surface and  $N$  the total  
264 reaction orthogonal to the sliding surface. Behavior of the soil can be considered undrained or drained. In the  
265 first case, undrained material values are assumed, i.e. cohesion equal to the undrained shear strength and null  
266 angle of friction. In the second case, effective values for cohesion and angle of friction are considered and  $N$   
267 transforms into  $N'$  to indicate effective total reaction.

268 The method of slices requires previously defining the sliding surface (normally assumed to be circular).  
269 Since that is unknown, normally a grid of centers is defined and the factor of safety is computed for each of  
270 the resulting circle and the slope safety factor will correspond with the minimum value. Moreover, the  
271 equation system obtained once the equilibrium is established on each slice is normally solved assuming  
272 different simplifications and hypotheses. The main ones typically used in Geotechnical Engineering are  
273 Bishop (1955) and Janbu (1954) methods. The former establishes the equilibrium of vertical forces and  
274 bending moments, assumes a horizontal resultant of the interslice forces and does not take into account  
275 interslice shear forces. The latter establishes the equilibrium of both horizontal and vertical forces, assumes a  
276 horizontal resultant of the interslice forces, and uses an empirical correction factor to account for interslice  
277 shear forces. Normally both methods are computed and the lower safety factor obtained is selected.

278 The described method can be easily extrapolated to a soil consisting of several horizontal materials just by  
279 adding the available shear strength developed by each material crossed by the sliding surface.

280 The model built for studying the slope stability of the Amherst wall by limit equilibrium methods is showed  
281 in **Fig. 6**. It should be noted that the model was geometrically similar to the one used in the finite element  
282 simulation. An area of 16x16 m was modelled, placing the nailed wall at 4.6 m from the left border of the  
283 model. Nails were introduced in the model as passive elements, with no tension force applying on them, and  
284 located at their real position, with an inclination of 20° and with an out-of-plane spacing equal to 1.5 m.  
285 Tensile capacity was set to 118 kN (equal to the maximum axial load of a bar of diameter 19 mm and yield  
286 stress 414 MPa) and bond strength was left as default value (15 kN/m). The shotcrete face was not modelled,  
287 as it is usual done when working with limit equilibrium methods, since its contribution to the stability of the

288 slope is normally negligible. As done in the case of the finite element simulation, the ground was stratified  
 289 each meter until reaching 5 m and then considered uniform.



290  
 291 *Fig. 6. Limit equilibrium method model developed for studying the Amherst wall (dimensions in m).*

292 *Results*

293 **Table 2** shows the mechanical characteristics of the different ground materials layers obtained after a trial  
 294 and error process in the finite element simulation, so as to attain a behavior of the numerical nailed wall  
 295 similar to the experimental one observed.

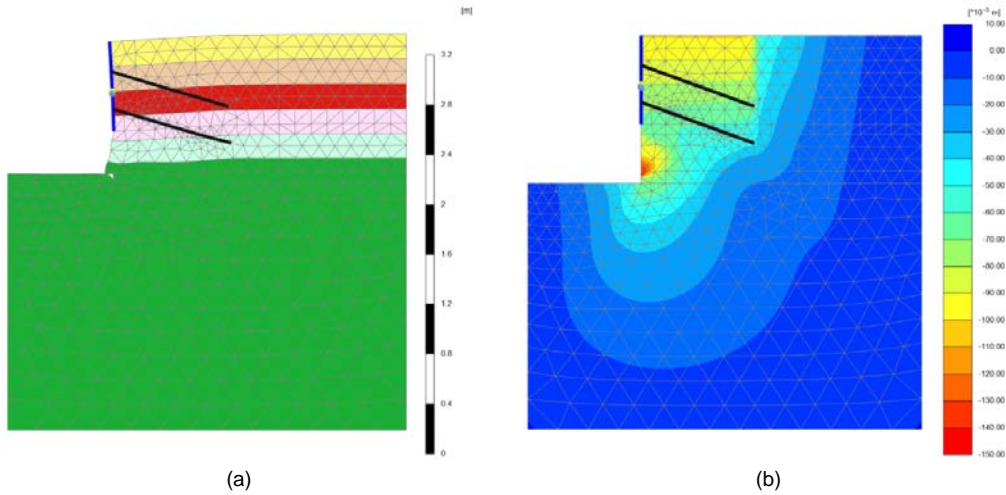
296 *Table 2. Mechanical characteristics of the ground materials.*

Stratum depth (m)	Mechanical model	Drain Behavior	$s_u$ (kPa)	$c'$ (kPa)	$\phi'$ (°)	$\psi$ (°)	$E$ (kPa)	$\nu$	$E_{50}$ (kPa)	$E_{ur}$ (kPa)	$E_{oed}$ (kPa)
0 – 1	Mohr-Coulomb	Drained	-	10	20	0	30000	0.33	-	-	-
1 – 2	Mohr-Coulomb	Drained	-	100	25	0	50000	0.33	-	-	-
2 – 3	Mohr-Coulomb	Drained	-	80	25	0	38000	0.33	-	-	-
3 – 4	Mohr-Coulomb	Drained	-	50	25	0	30000	0.33	-	-	-
4 – 5	Hardening Soil	Undrained	39	-	-	0	-	-	26000	52000	26000
5 –	Hardening Soil	Undrained	27	-	-	0	-	-	16000	32000	16000

297 In order to ensure the failure of the slope in the finite element model, the overexcavation stage was divided  
 298 into two stages: one stage where all but the last 0.25 m were excavated and a second stage where those last  
 299 0.25 m were excavated. Based on this, with the proposed geotechnical materials of **Table 2** a numerical  
 300 instability of the solving procedure occurred when trying to excavate the final 0.25 m, not finding  
 301 convergence and registering a negative total stiffness of the model. This means that failure of the wall took  
 302

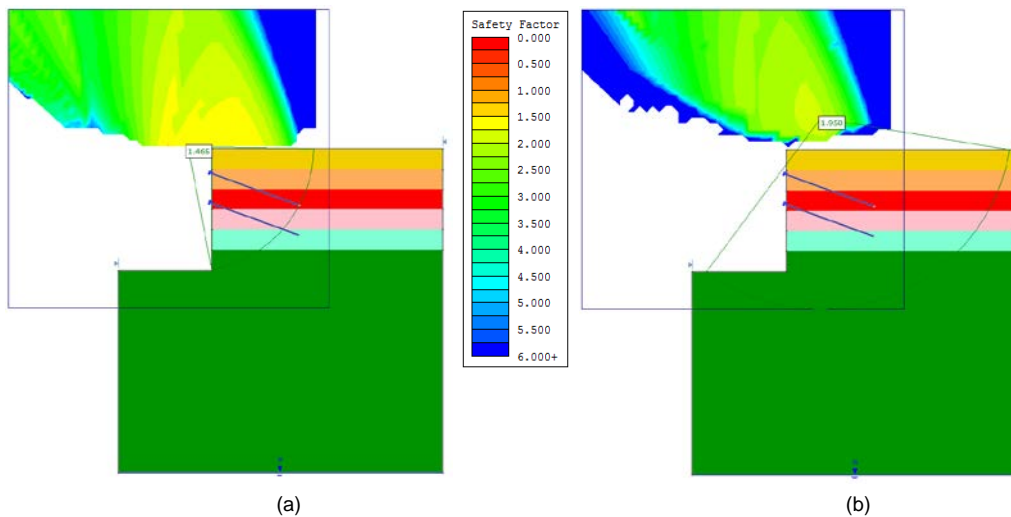


303 place. **Fig. 7** shows the deformed shape (**Fig. 7a**) and lateral displacements (**Fig. 7b**) obtained for this final  
 304 stage. As can be seen, displacement of the wall follows the same behavior observed in the experimental test  
 305 and the lateral displacements at the top of the model are about 10 cm, as recorded by the inclinometers  
 306 experimentally.



307 (a) (b)  
 308 *Fig. 7. Numerical study of the Amherst wall by a finite element model: (a) deformed shape; (b) lateral*  
 309 *displacements.*

310 The limit equilibrium method model developed was also run using the proposed geotechnical materials. **Fig.**  
 311 **8** shows safety factor obtained for both the Bishop (1955) and Janbu (1954) methods (**Figs. 8a and 8b**,  
 312 respectively), being the lowest one that obtained by the Bishop method and equal to 1.47.



313 (a) (b)  
 314 *Fig. 8. Numerical study of the Amherst wall by limit equilibrium methods: (a) factor of safety based on*  
 315 *Bishop method; (b) factor of safety based on Janbu method.*



316 **Analysis of the results and discussion**

317 *Ground modelling*

318 Results obtained in the back analysis of the Amherst wall showed that numerically the ground can be  
319 separated in two different zones: an upper zone, corresponding to the first 4 m, and a lower one, which  
320 extends below, from a depth of 4 m.

321 The upper zone contains the first four ground numerical strata, and approximately corresponds to the area  
322 where the shotcrete face existed. In this zone ground materials were modelled as drained materials working  
323 according to the Mohr-Coulomb mechanical model. This drained behavior may be explained by two main  
324 aspects: (a) the experimental displacement observed on the wall, which rotated by its lower point towards the  
325 excavation, a typical performance of granular materials; and (b) the geotechnical characteristics of the upper  
326 layers of the soil according to the geotechnical investigation of the area which is composed by a mix of sand,  
327 silt and clay, with a slightly high OCR. Besides, it should be mentioned that since geological-geotechnical  
328 profile indicated that surface material corresponded to a fill, mechanical characteristics of the first numerical  
329 layer were selected based on typical values of a fill (Sánchez-Alciturri et al. 1993).

330 The lower zone comprises the last two ground strata, and corresponds to the area where the overexcavation  
331 was conducted. In this zone ground materials were modelled as undrained materials working according to the  
332 Hardening Soil mechanical model. This numerical approach considers that materials in this zone behave as  
333 cohesive ones, which is consistent with the geological-geotechnical characterization of the Amherst wall  
334 area, composed by a mix of silt and clay from a depth of around 4 m. Besides, since excavation was carried  
335 out fast in terms of time (no more than 15 days passed between the start of excavation of the top part of the  
336 wall and the failure of the nailed wall due to the overexcavation) an undrained behavior may be expected. It  
337 should be clarified that materials in the upper zone (modelled by the Mohr-Coulomb mechanical model) may  
338 also be working under an undrained behavior according to this, but since those materials were found to  
339 numerically behave as granular materials, a drained behavior was selected.

340 Having found a better performance of the use of the Hardening Soil mechanical model to simulate the  
341 cohesive soil strata of the ground which are located on the bottom of the excavation, is in accordance with  
342 the work of Singh and Sivakumar Babu (2010) who compared the use of the Mohr-Coulomb and the  
343 Hardening Soil models in simulating a soil nailed wall and observed that the former overestimated (Callisto

344 et al. 1999; Brinkgreve et al. 2006) the base heave of the excavation face to almost twice as that predicted by  
345 the latter. This phenomenon is of importance, since, as stated by the FHWA (2003), basal heave may be a  
346 failure mode of soil nailed walls caused by the unbalanced forces that appear on the bottom of the excavation  
347 which may result in a bearing capacity failure of the ground.

348 All the aforementioned concerns regarding the convenience of the use of a certain mechanical model for  
349 defining the geotechnical materials and thus simulating as close as possible the real behavior of the nailed  
350 wall are the keystone of a good finite element model. However, it is interesting to note that in terms of a  
351 design based on the limit equilibrium method, those aspects are of a lower importance. As showed above, the  
352 objective of limit equilibrium methods is computing the safety factor, which only involves those forces that  
353 contribute to stabilize the system and those that tend to make it unstable.

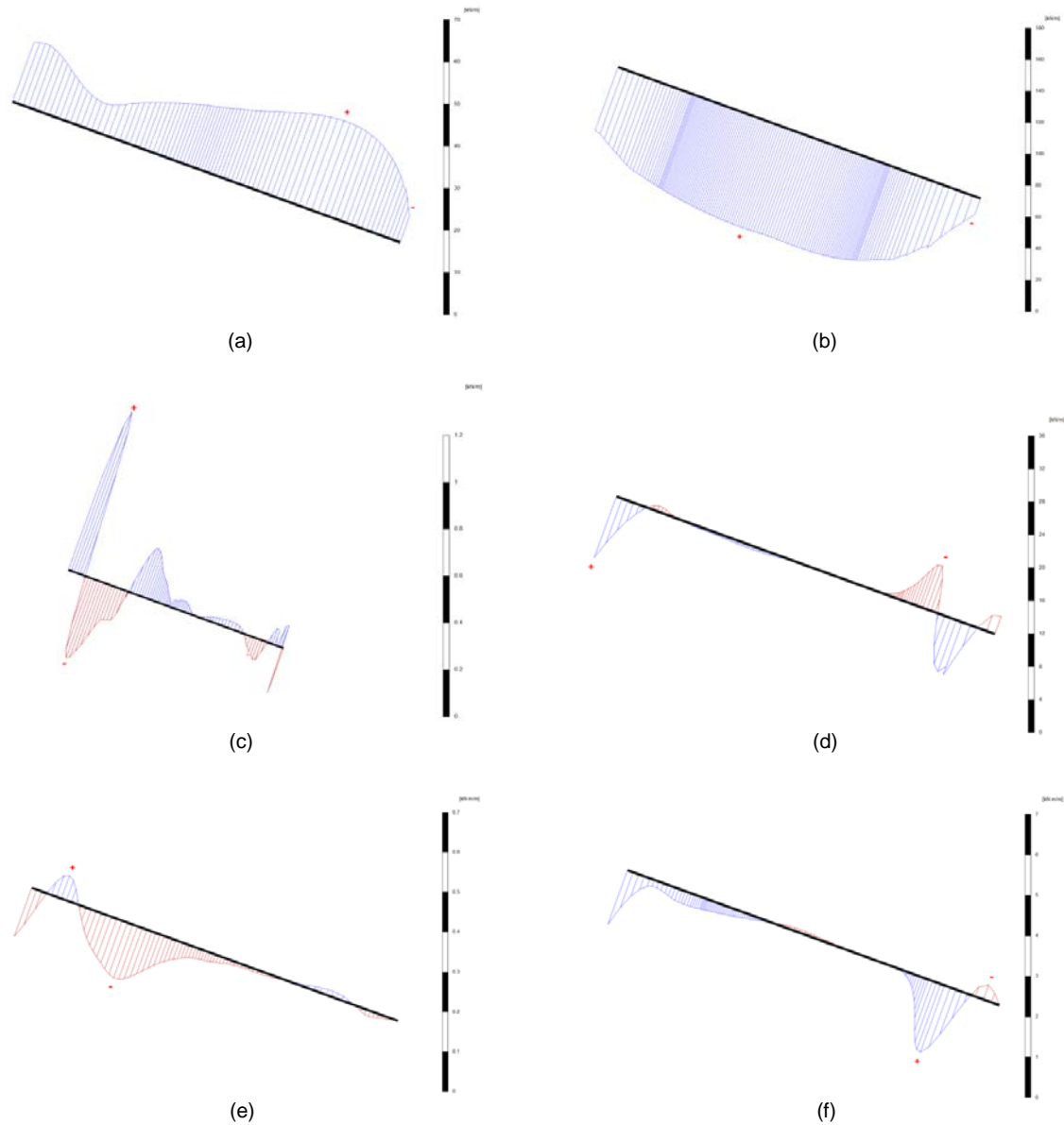
354 This is a great advantage of the limit equilibrium methods, since (aside parameters regarding to the nails)  
355 only ground strength properties are needed, i.e. angle of friction and cohesion (or undrained shear strength  
356 when simulating an undrained cohesive soil). That simplifies greatly the problem and allows a fast and  
357 efficient designing of soil nailed walls, avoiding the necessity of using geotechnical properties like the elastic  
358 moduli of the ground materials, which are normally difficult to obtain. Nevertheless, one should keep in  
359 mind that the real behavior of the soil and the wall is neglected and that the whole performance of a nailed  
360 wall is reduced to a unique number (the safety factor), which may be problematic in some cases, especially  
361 when excessive ground deformations are developed.

#### 362 *Load distribution on nails*

363 An important aspect when designing a soil nailing wall is related with the load distribution on nails. As seen  
364 in the literature (Fan and Luo 2008; Wei and Cheng 2010), nails located in the lower part of a soil slope have  
365 a considerable influence on the overall stability of the system, and consequently they tend to absorb more  
366 loads. In those lower rows, the highest values of shear forces and bending moments are normally located at  
367 sections close to the nails ends.

368 Those issues were captured by the numerical simulation developed by the finite element model. **Fig. 9** shows  
369 load distribution on nails at the moment of failure of the soil nailing wall. As can be observed, axial loads  
370 clearly reached higher values in the lower row of nails: a value about 22.5 kN/m was obtained in the upper  
371 row (**Fig. 9a**) while more than three times, nearly 69.0 kN/m, was obtained in the lower row (**Fig. 9b**). A

372 similar phenomenon was observed for the shear loads, with a value of about 0.65 kN/m recorded as  
 373 maximum shear load in the upper row (**Fig. 9c**) and approximately a value of 5.5 kN/m in the lower row  
 374 (**Fig. 9d**). Finally in terms of bending moments, maximum value in the upper row was about 0.14 kN·m/m  
 375 (**Fig. 9e**), and 1.75 kN·m/m in the lower row (**Fig. 9f**). Thus, higher loads were developed in the lower row  
 376 of nails, and in that row the load distribution graphs show that, as expected, highest values of shear forces  
 377 and bending moments occur at a great distance from the wall (in the vicinity of the end of the nails).



378  
 379 *Fig. 9. Load distribution on the nails obtained by the finite element model developed in the moment of*  
 380 *failure: (a) axial load in the upper row of nails; (b) axial load in the lower row of nails; (c) shear force in*  
 381 *the upper row of nails; (d) shear force in the lower row of nails; (e) bending moment in the upper row of*  
 382 *nails; (f) bending moment in the lower row of nails.*

383 When using limit equilibrium methods, maximum tension within nails is normally considered to be at the  
384 intersection of such elements with the failure surface (Wei and Cheng 2010). Even though this is a clear  
385 simplification, it is interesting to observe that the potential slip surface defined by limit equilibrium methods  
386 run in this work (see **Fig. 8**) crosses the lower row of nails near their end. Besides, the axial load distribution  
387 obtained for those nails (**Fig. 9b**) shows that axial load tend to achieve a certain value along a part of the nail  
388 and that value is kept constant until reaching the vicinity where the highest values of shear forces and  
389 bending moments appear (near the end of the nails).

390 Thus, the use of the classical approach of many practitioners, who assume that the maximum tensile force  
391 line matches the potential sliding surface obtained by limit equilibrium methods, may be used to estimate the  
392 loads of nails. Those elements can therefore be designed considering that the mass of soil inside of the  
393 sliding surface (close to the wall) tends to pull the nail out of the ground, while the mass out of the sliding  
394 surface tends to restrain the nail from being pulled out (FHWA 1996; Wei and Cheng 2010).

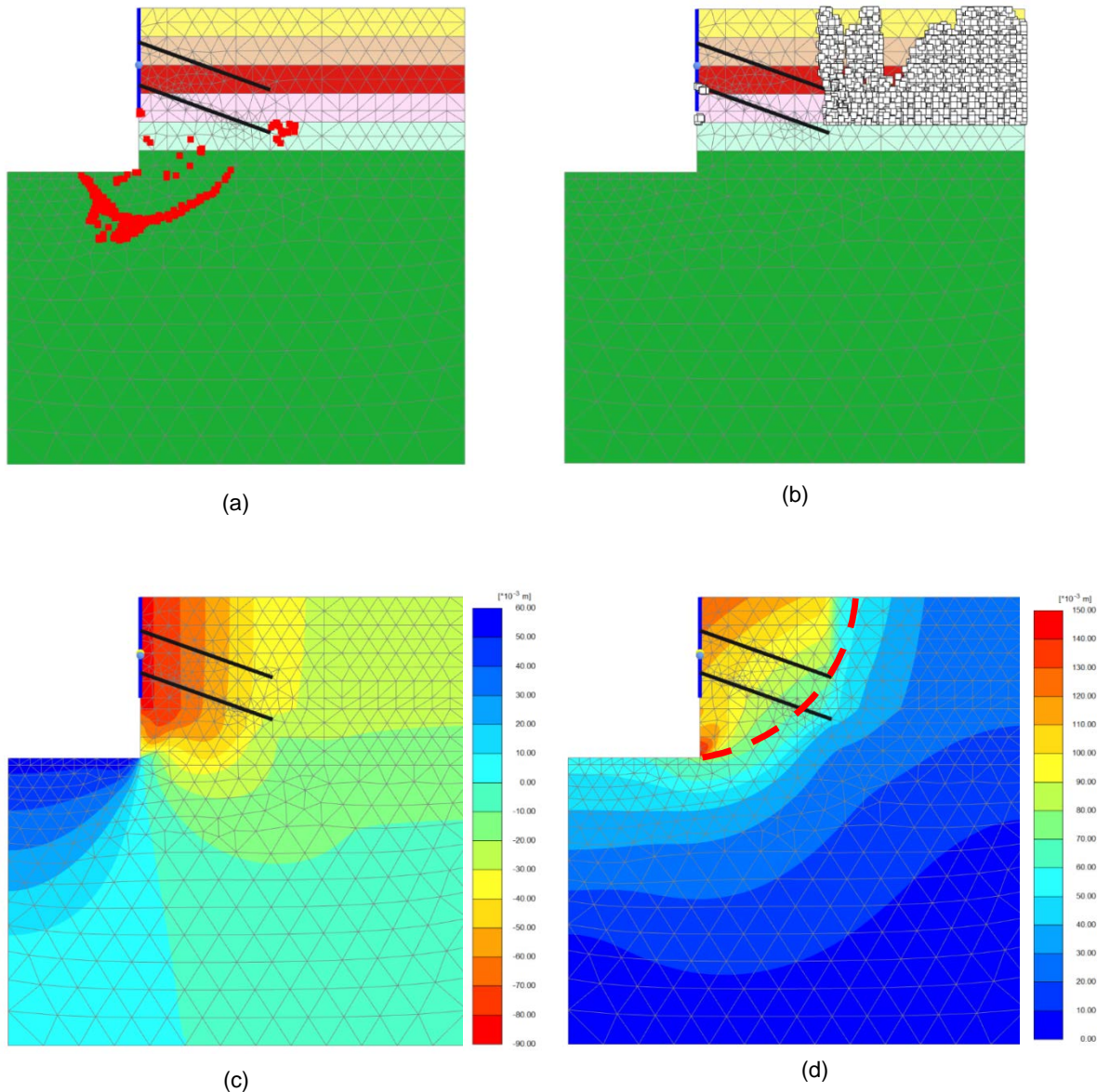
#### 395 *Failure and ground deformations*

396 Strictly speaking, if the safety factor obtained by a limit equilibrium method is above 1.0 the slope may be  
397 considered not to be in a failure state. The lowest safety factor obtained in the Amherst wall model was 1.47,  
398 so, at first one may think that the system is in a safe situation. However, as the finite element model  
399 demonstrated, the system is in a failure condition.

400 **Figs. 10a** and **10b** display tension cut-off points and failure points given by the finite element model  
401 developed at the step when no convergence of the model was attained and a negative total stiffness was  
402 obtained, i.e. when failure was considered to occur. As can be observed, failure points occur mainly at the  
403 undrained cohesive materials located in the lower zone of the soil nailed wall, while tension cut-off points  
404 are generally located in the upper zone of the wall and to a certain distance to it, being a consequence of the  
405 lateral movement experimented by the wall (which rotates by its lower point towards the excavation).

406 Hence, assuming that in a soil nailed wall a safety factor equal to 1.0 means no failure may be not correct. In  
407 fact, in slope stability, due to the own nature of the calculation methods (especially the limit equilibrium  
408 methods) and the reliability of the geotechnical parameters, according to geotechnical codes, a safety factor  
409 lower than 1.2 - 1.5 (the value may depend on issues such as the permanent or temporary conditions of the  
410 work and the contemplation of the seismic action) should be considered an unsafe situation. Soil nailing can

411 be seen as a particular case of slope stability, so taking into the results obtained in the numeric simulation  
412 undertaken, a safety factor of at least 1.5 should be ensured when using limit equilibrium methods to design  
413 a soil nailed wall.



414  
415 *Fig. 10. Finite element model results: (a) Tension cut-off points; (b) Failure points; (c) vertical ground*  
416 *deformations; (d) total ground deformations (depicted in red Bishop's failure circle according to the limit*  
417 *equilibrium method developed).*

418 Besides mentioned issues concerning failure of the system, as was indicated above, limit equilibrium  
419 methods neglect deformations, which may be problematic if excessive ground deformations are developed.  
420 **Fig. 10c** shows vertical deformations of the ground obtained in the finite element model developed prior to  
421 failure. Values exhibited in the vicinity of the excavation are larger than one inch (2.54 cm), the value

422 typically considered to be the maximum settlement that does not induce any deformation problems to  
423 infrastructures and buildings. **Fig. 10d** displays ground total deformations. Values of more than 10 cm are  
424 recorded, which likely may lead to compromise the own stability of the excavation.

425 Thus, both graphs demonstrate that in the case under study excessive ground deformations take place, which  
426 can never be detected by just using limit equilibrium methods. However, it should be noted that limit  
427 equilibrium methods are able of capturing with relative approximation the failure surface (see **Fig. 10d**).  
428 That, together with the advantages showed above for those methods (easy to build models, not many  
429 geotechnical properties involved, fast and simple estimation of nail forces) make limit equilibrium methods a  
430 very useful tool to design soil nailed walls. However, in a second phase, once the main parameters of the  
431 design are defined (such as excavation phases and nail strength properties) a finite element model should be  
432 developed in order to verify the good performance of the soil nailed wall and especially to check the  
433 possibility of having excessive ground deformations.

#### 434 **Conclusion**

435 This paper has tried to establish the convenience of the applicability of limit equilibrium methods and finite  
436 element models for designing soil nailed walls, considering both the suitability of an easy and fast design  
437 process, and the necessity to take into account issues such as ground deformations to avoid problematic  
438 consequences that can arise during their execution phase and service life.

439 For doing this, a numerical study of the Amherst wall was performed and subsequently analyzed. The  
440 Amherst wall is a full-scale soil nailed wall built as an experimental test at the Amherst National  
441 Geotechnical Experimentation Site, near the town of Amherst, Massachusetts, and it intentionally failed due  
442 to an overexcavation.

443 A finite element model and a limit equilibrium model (using the method of the slices) were developed. Nails  
444 and shotcrete were placed at the same positions as where located in the experimental test and, as a  
445 consequence of the variability of the ground characteristics at the depths where the wall was built, the soil  
446 was numerically stratified each meter until reaching one meter before the total excavation. A back-analysis  
447 procedure was used to define the mechanical properties of each ground stratum, validating the values with  
448 the behavior of the Amherst wall experimentally observed.

449 In the numerical model, the ground is divided into an upper zone, corresponding approximately to the area  
450 where the shotcrete face existed, and a lower one, where the overexcavation was conducted. The upper zone  
451 was found to behave similar to a granular material, causing the nailed wall to rotate by its lower end and  
452 producing the highest value of lateral deformation at its top part, while the lower zone was found to behave  
453 as an undrained cohesive material. Thus, this paper has also shown an approach to numerically model soil-  
454 nailed walls in ground situations where the soil is neither pure cohesive nor pure granular, but a mix of them.  
455 Materials more similar to granular soils have demonstrated to behave according to a Mohr-Coulomb model  
456 (with drained analysis), while materials more similar to cohesive soils are better reproduced using the  
457 Hardening Soil model (with undrained analysis).

458 Limit equilibrium methods have showed to be fast and efficient when designing soil nailed walls, presenting  
459 several advantages of their use. The main one may probably be the fact that they are focused on computing  
460 the safety factor, which involves only forces, simplifying greatly the problem and avoiding the necessity of  
461 using geotechnical properties difficult to obtain such as the elastic moduli of the ground materials (for limit  
462 equilibrium methods only ground strength properties, i.e. angle of friction and cohesion are needed).  
463 Moreover, they allow a good estimation of the tensile stresses to which the nails are subjected by assuming  
464 that the maximum tensile force line matches the potential sliding surface obtained by those methods.

465 Design of a soil nailed wall by limit equilibrium methods should be addressed with some caution, however.  
466 Firstly they do not take into account ground deformations, so they do not detect the development of  
467 excessive ground deformations. Secondly a safety factor of 1.0 or a little higher may not be a reliable  
468 indicator of a good performance of the wall. It is recommendable to reach at least a safety factor of 1.5 in  
469 order to consider that the system designed is in a safe situation.

470 On the other hand finite element methods allow a good determination of both performance of the nailed wall  
471 and development of ground deformations. They also give more information about stresses developed in the  
472 nails, not limiting the output value to axial loads, but delivering the value of shear loads and bending  
473 moments that can appear in those elements. Nevertheless finite element methods require more parameters  
474 than limit equilibrium methods to be properly defined (both strength and deformability properties of ground  
475 materials are needed) as well as the selection of the appropriate mechanical model (e.g. Mohr-Coulomb or  
476 Hardening Soil) to correctly simulate the soil behavior. That results in more complex model, but if they are

477 adequately built they will provide good information about the expected behavior of the soil both in the  
478 excavation and its surroundings.

479 After having conducting the analysis and comparison of both limit equilibrium methods and finite element  
480 methods, a designing process for soil nailed walls based on two steps or phases is proposed. In a first phase  
481 limit equilibrium methods may be used to define the main parameters of the design such as the depth of  
482 excavations, the nail strength properties and a global safety factor fulfilment. Then, in a second phase, a  
483 finite element model should be developed to verify the good performance of designed system, to account for  
484 the real forces expected to be developed in the nails (axial loads, shear loads and bending moments) and to  
485 check the possibility of having excessive ground deformations that can give rise to problems in surrounding  
486 buildings and structures as well as endanger the safety of the own excavation.

#### 487 **Acknowledgements**

488 This research did not receive any specific grant from funding agencies in the public, commercial, or not-for-  
489 profit sectors.

#### 490 **References**

- 491 Al-Hussaini, M.M and Johnson, L.D. (1978). Numerical analysis of reinforced earth wall. *Proc. ASCE*  
492 *Symposium on Earth Reinforcement*, 98-126, Pittsburgh, PA.
- 493 Beim, J. and Luna S.C. (2012). “Results of dynamic and static load tests on helical piles in the varved clay of  
494 Massachusetts”. *DFI Journal, Deep Foundations Institute*, 6, 58–67.
- 495 Bishop, A.W. (1955). “The use of slip circle in the stability analysis of slopes”. *Geotechnique*, 5, 1-17.
- 496 Brigham-Grette, J., Rittenour, T., Stone, J., Ridge, J., Werner, A., Levy, L., Dincauze, D., Klekowski, E. and  
497 Little, R. (2000). “A Drainage History for Glacial Lake Hitchcock: Varves, Landforms, and Stratigraphy”.  
498 In: J. Brigham-Grette (Ed.), *North Eastern Friends of the Pleistocene Field Guidebook*, Dept. of Geosciences  
499 Contribution No. 7, University of Massachusetts, Amherst, MA., 125 pp.
- 500 Brinkgreve, R.B.J., Bakker, K.J. and Bonnier, P.G. (2006). “The relevance of small-strain soil stiffness in  
501 numerical simulation of excavation and tunneling projects”. *Proc. 6th European Conference in Geotechnical*  
502 *Engineering*, Graz, Austria.



503 Callisto, L., Amorosi, A. and Rampello, S. (1999). “The influence of pre-failure soil modelling on the  
504 behaviour of open excavations”. *Proc. 12th European Conference on Soil Mechanics and Geotechnical*  
505 *Engineering*, Amsterdam, The Netherlands.

506 DeGroot, D. and Lutenecker, A.J. (1994). “A comparison between field and laboratory measurements of  
507 hydraulic conductivity in a varved clay”. In: D.E. Daniel, S.J. Trautwein (Eds.), *Hydraulic Conductivity and*  
508 *Waste Contaminant Transport in Soil*, American Society for Testing and Materials Special Technical  
509 Publication No. 1142, pp. 300–317.

510 DeGroot, D.J. and Lutenecker, A.J. (2005). “Characterization by Sampling and In Situ Testing - Connecticut  
511 Valley Varved Clay”. *Stud. Geotech. Mech.*, 27, 107–120.

512 Ehrlich, M. and Silva R. C. (2015). “Behavior of a 31m high excavation supported by anchoring and nailing  
513 in residual soil of gneiss”. *Eng. Geol.*, 191, 48–60.

514 Fan, C.C. and Luo, J.H. (2008). “Numerical study on the optimum layout of soil nailed slopes”. *Comput.*  
515 *Geotech.*, 35, 585–599.

516 FHWA (1996). *Manual for design and construction monitoring of soil nail walls*. Report FHWA-SA-96-069,  
517 US Department of Transportation, Federal Highway Administration, Washington DC.

518 FHWA (2003). *Geotechnical engineering circular No 7—soil nail walls*. Report FHWA0-IF-03-017. US  
519 Department of Transportation, Federal Highway Administration, Washington DC.

520 Ghareh, S. (2015). “Parametric assessment of soil-nailing retaining structures in cohesive and cohesionless  
521 soils”. *Measurement*, 73, 341–351.

522 Holman, T.P. and Tuozzolo, T.J. (2009). “Load Development in Soil Nails from a Strain-Gauge  
523 Instrumented Wall”. In: M. Iskander, D.F. Laefer, M.H. Hussein (Eds.), *Contemporary topics in deep*  
524 *foundations: proceedings of selected papers of the 2009 International Foundation Congress and Equipment*  
525 *Expo, March 15-19, 2009, Orlando, Florida*, Geotechnical Special Publication No. 185, ASCE, Reston, Va.,  
526 pp. 25–32.

527 Janbu, N. (1954). “Application of composite slip surfaces for stability analysis”. *Proc. European Conference*  
528 *on Stability of Earth Slopes*, Stockholm, 3, 43–49.

529 Junaideen, S.M., Tham, L.G., Law, K.T., Lee, C.F. and Yue, Z.Q. (2004). “Laboratory study of soil nail  
530 interaction in loose completely decomposed granite”. *Can. Geotech. J.*, 41, 274–286.

531 Kim, J.S. Kim, J.Y., and Lee, S.R. (1997). “Analysis of soil nailed earth slope by discrete element method”.  
532 *Comput. Geotech.*, 20, 1–14.

533 Liew, S.S., and Khoo, C.M. (2006). “Soil nail stabilisation for a 14.5 m deep excavation at uncontrolled fill  
534 ground”. *Proc. 10th International Conference on Piling and Deep Foundations*, Amsterdam, The  
535 Netherlands.

536 Liu J., Shang, K. and Wu, X. (2016). Stability Analysis and Performance of Soil-Nailing Retaining System  
537 of Excavation during Construction Period. *J. Perform. Constr. Facil.*, 30(1), C4014002.

538 Oral, T. and Sheahan, T.C. (1998). “The use of soil nails in soft clays” .In: R.J. Finno, Y. Hashash, C.L. Ho,  
539 B.P. Sweeney (Eds.), *Design and construction of earth retaining systems*, Geotechnical Special Publication  
540 No. 83, ASCE, Reston, Va., pp. 26–40.

541 PLAXIS (2016) [Computer software]. Plaxis full manual. Delft, The Netherlands.

542 Plumelle, C., Schlosser, F., Delage, P. and Knochenmus. G. (1990). “French national research project on soil  
543 nailing: Clouterre”. In: P.C. Lambe, L.A. Hansen, (Eds.), *Design and performance of earth retaining*  
544 *structures*, Geotechnical Special Publication No. 25, ASCE, Reston, Va., pp. 660–675.

545 Pradhan, B., Tham, L.G., Yue, Z.Q., Junaideen, S.M. and Lee, C.F. (2006). “Soil-nail pullout interaction in  
546 loose fill materials”. *Int. J. Geomech.* ASCE 6, 238–247.

547 Ridge, J.C., Balco, G., Bayless, R.L., Beck, C.C., Carter, L.B., Dean, J.L., Voytek, E.B. and Wei, J.H.  
548 (2012). “The new North American varve chronology: a precise record of southeastern Laurentide ice sheet  
549 deglaciation and climate, 18.2-12.5 kyr BP, and correlations with Greenland ice core records”. *Am. J. Sci.*,  
550 312, 685–722.

551 Ridge, J.C. and Larsen, F.D. (1990). “Re-evaluation of Antevs’ New England varve chronology and new  
552 radiocarbon dates of sediments from glacial Lake Hitchcock”. *Geol. Soc. Am. Bull.*, 102, 889–899.

553 Sánchez-Alciturri, J.M., Palma, J., Sagaseta, C. and Cañizal, J. (1993). “Mechanical properties of wastes in  
554 sanitary landfill”. *Proc. of the Green’93 Symposium, Geotechnics related to the environment*, Bolton, UK.

555 Schanz, T., Vermeer, P.A. and Bonnier, P.G. (1999). “The hardening soil model – formulation and  
556 verification”. *Proc. Plaxis Symposium on Beyond 2000 in Computational Geotechnics*, Amsterdam, The  
557 Netherlands.

558 Seo, H.J., Lee, I.M. and Lee, S.W. (2014). “Optimization of Soil Nailing Design Considering Three Failure  
559 Modes”. *KSCE J. Civ. Eng.*, 18, 488-496.

560 Sheahan, T. C. (2000). “A field study of soil nails in clay at the University of Massachusetts - Amherst  
561 National Geotechnical Experimentation Site”. In: J. Benoit, A.J. Lutenegeger (Eds.), *National geotechnical  
562 experimentation sites*, Geotechnical Special Publication No. 93, ASCE, Reston, Va., pp. 250–263.

563 Sheahan, T.C. and Ho, C.L. (2003). “Simplified Trial Wedge Method for Soil Nailed Wall Analysis”. *J.  
564 Geotech. Geoenviron. Eng.*, 129, 117–124.

565 Shiu, Y.K. and Chang, G.W.K. (2006). “Effects of inclination, length pattern and bending stiffness of soil  
566 nails on behavior of nailed structures.” GEO Report No.197. Geotechnical Engineering Office. Hong Kong.

567 Singh, V.P. and Sivakumar Babu, G.L. (2010). “2D Numerical Simulations of Soil Nail Walls”. *Geotech.  
568 Geol. Eng.*, 28, 299–309.

569 Sivakumar Babu, G.L., Murthy, B.R.S. and Srinivas A. (2002). “Analysis of construction factors influencing  
570 the behavior of soil nailed earth retaining walls”. *Ground Improvement*, 6, 137–143.

571 Slide (2016) [Computer software]. *Slide Manual*. RocScience, Inc. Toronto, Canada.

572 Smith, I.M. and Su, N. (1997) “Three dimensional finite element analysis of nailed soil wall curved in plan”.  
573 *Int. J. Numer. Anal. Met. Geomech.*, 21, 583–597.

574 Stone, J.R. and Ashley, G.M. (1995). “Timing and mechanisms of glacial Lake Hitchcock drainage”.  
575 *Geological Society of America Abstracts with Programs*, 27, 85.

576 Stone, J.R., Schafer, J.P., London, E.H., Lewis, R.L., DiGiacomo-Cohen, M.L. and Thompson, W.B. (1998).  
577 “Quaternary geologic map of Connecticut and Long Island Sound Basin (scale 1:175,000)”. *U.S. Geological  
578 Survey Open-File Report*, 98–371, 1 sheet, 77 p.

579 Su, L.J., Chan, T.C.F., Shiu, Y.K., Cheung, T. and Yin, J.H. (2007). “Influence of degree of saturation on  
580 soil nail pull-out resistance in compacted completely decomposed granite fill”. *Can. Geotech. J.*, 44, 1314–  
581 1328.

582 Tan, Y., Li, X., Kang, Z., Liu, J. and Zhu, Y. (2015). “Zoned Excavation of an Oversized Pit Close to an  
583 Existing Metro Line in Stiff Clay: Case Study”. *J. Perform. Constr. Facil.*, 29(6), 04014158.

584 Thorson, R.M., Forrest, D. and Jones, B. (2014). “Alluvial Archaeology: A stratigraphic model for  
585 postglacial archaeology in the Connecticut River Valley. Hydraulic back-flood model for the archaeological  
586 stratigraphy of the Connecticut River Alluvial Lowland, central Connecticut, USA”. *Quat. Int.*, 342,173–  
587 185.

588 Unterreiner, P., Benhamida, B. and Schlosser, F. (1997). “Finite element modelling of the construction of a  
589 full-scale experimental soil-nailed wall, French National Research Project CLOUTERRE”, *J. Ground*  
590 *Improvement*, 1, 1–8.

591 Wei, W.B. and Cheng, Y.M. (2010). “Soil nailed slope by strength reduction and limit equilibrium methods”.  
592 *Comput. Geotech.*, 37, 602–618.

593 Wood, T.A., Jayawickrama, P.W. and Lawson, W.D. (2009). “Instrumentation and Monitoring of an  
594 MSE/Soil Nail Hybrid Retaining Wall”. *Proc. Int. Foundation Congress and Equipment Expo.* ASCE,  
595 Orlando, Fl.

596 Woods R. D. (1995). “National Geotechnical Experimentation Sites (NGES)”. *Proc. of the Third*  
597 *International Conferences on Recent Advances in Geotechnical Earthquake Engineering and Soil Dynamics*,  
598 *April 2-7, 1995, Volume III*, St. Louis, Missouri, 1457–1464.

599 Xue, X., Yang, X. and Liu, E. (2013). “Application of modified Goodman model in soil nailing”. *Int. J.*  
600 *Geomech.* ASCE, 13, 41–48.

601 Yin, J.H. and Su L.J. (2006). “An innovative laboratory box for testing nail pull-out resistance in soil”.  
602 *ASTM Geotech. Test. J.*, 29, 1–11.

603 Yuan, J. X., Yang, Y., Tham, L.G., Lee, P.K.K. and Tsui, Y. (2003). “New Approach to Limit Equilibrium  
604 and Reliability Analysis of Soil Nailed Walls”. *Int. J. Geomech.* ASCE, 3, 145–151.

605 Zhang, M., Song, E. and Chen, Z. (1999). “Ground movement analysis of soil nailing construction by three-  
606 dimensional (3-D) finite element modeling (FEM)”. *Comput. Geotech.*, 25, 191–204.

607